as the dotted line in Figure 3a. Considering the uncertainties involved, particularly in t_c as the pressure is increased to above 1 micron, the agreement is quite good.

The rates of unimolecular decomposition of the complex both in the forward direction (eq 7) and the backward direction (eq 6) were calculated as a function of relative kinetic energy by the familiar Rice-Ramsberger-Kassel-Marcus theory.[23] This calculation, which was similar to that reported by Allen and Lampe,[12] indicates that with a Gaussian kinetic energy distribution of 0.3-eV width in the reactant ions, unstabilized collision complexes will be directly observable ($\tau_0 \geq 10^{-6}$ s in our apparatus) only for laboratory energies of SiH_3^+ below 1.4 eV (LAB). The fact that Allen and Lampe[12] observed unstabilized collision complexes at energies up to 2 eV (LAB) is to be attributed to the much wider kinetic energy spread in their SiH_3^+ ion beam.

(23) Robinson, P. J.; Holbrook, K. A. "Unimolecular Reactions"; Wiley-Interscience: New York, 1972; Chapters 4 and 5.

Acknowledgment. This research was supported by the U.S. Department of Energy under Contract DE-AS02-76ER03416. Thanks are also due to the Education Committee of the Gulf Oil Corp. for a grant that assisted in the construction of the apparatus.

Infrared Spectrum of the Primary Ozonide of Ethylene in Solid Xenon

Christopher K. Kohlmiller and Lester Andrews*

Contribution from the Chemistry Department, University of Virginia, Charlottesville, Virginia 22901. *Received October 27, 1980*

Abstract: Separate Xe/O_3 and Xe/C_2H_4 mixtures were condensed on a CsI window at 50 K and then warmed to 80–100 K. Strong infrared absorptions due to the secondary ozonide and weaker bands at 409, 647, 727, 846, 927, 983, and 1214 cm^{-1} replaced the ethylene and ozone absorptions. The latter new bands agree with earlier solid film and CO_2 matrix studies and are assigned to the primary ozonide. Isotopic substitution ($^{16,18}O_3$, $^{18}O_3$, CH_2CD_2, C_2D_4, $^{13}C_2H_4$) provides a sound basis for vibrational assignments. A sextet splitting for the 647-cm^{-1} antisymmetric O–O–O stretching mode in the 50% oxygen-18 enriched experiment confirms the primary ozonide structure and directly characterizes the weak O–O–O single bonds.

The mechanism of the reaction between ozone and olefins has attracted considerable attention.[1-4] Bailey's recent monograph[1] contains an excellent comprehensive review of this work, including evidence supporting the initial step as a 1,3-dipolar cycloaddition to form a five-membered ring **1**. This mechanism was first

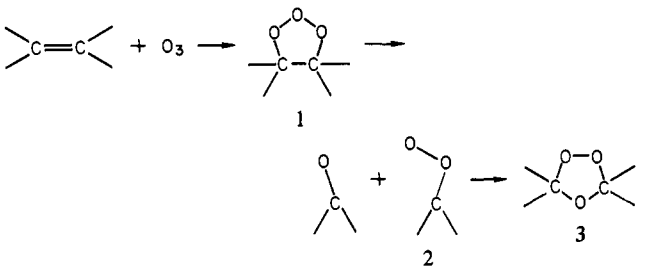

proposed by Criegee[2] in 1951. The 1,2,3-trioxolane, **1**, is known as the primary ozonide (POZ) and the 1,2,4-trioxolane, **3**, as the secondary ozonide (SOZ). The "Criegee intermediate", **2**, was thought to exist as the zwitterion in solution,[2] but it is probably a diradical or dioxirane in the gas phase.[5] The symmetric nature of the POZ structure was demonstrated by Bailey et al.[6] from the low-temperature (−110 and −95 °C) NMR spectrum of the *trans*-1,2-di-*tert*-butylethylene POZ. Other NMR studies by Durham and Greenwood[7] have supported the symmetric structure of the POZ and established that the POZ is an intermediate in the ozonolysis reactions. This is consistent with the 1,2,3-trioxolane structure but a π-complex cannot be eliminated. Such structures have been found with electron-rich systems, like aromatics,[2] and probably are formed at very low temperatures as precursors to the 1,2,3-trioxolane.[8-11]

Other authors have studied ozonolysis reactions by infrared spectroscopy. Hull et al.[8] deposited ozone and olefins (nine different compounds) separately onto a cold (−185 °C) window. After the window was warmed (−175 to 150 °C), two products were formed, presumably a π-complex and the 1,2,3-trioxolane (except C_2H_4 formed only the 1,2,3-trioxolane). After the window was further warmed, the π-complex decomposed, probably to the initial reactants, but the POZ gave the SOZ and other products. The formations of the POZ's of *trans*-di-isopropylethylene and of 2,4,4-trimethylpent-1-ene in the liquid phase have been observed by Alcock and Mile.[9,11] Of particular interest, Nelander and Nord have studied the POZ of ozone and ethylene in CCl_4 and CO_2 matrices.[12]

Previous workers made POZ vibrational assignments based on an ozone model, which cannot be accurate for the 1,2,3-trioxolane structure. This paper characterizes the ethylene POZ fundamentals, and the POZ itself, using carbon-13, oxygen-18, and deuterium isotopic data for the first time. A xenon matrix affords the inertness needed for isotopic purity and the temperature range required for reaction. Similar isotopic data for the SOZ structures and attempts to isolate the Criegee intermediate will be discussed in a future paper.

Experimental Section

Apparatus. The cryogenic refrigeration system and vacuum vessel have been previously described.[13] All spectra were recorded on a

(1) Bailey, P. S. "Ozonation in Organic Chemistry"; Academic Press: New York, 1978; Vol. I.
(2) Criegee, R. *Angew. Chem., Int. Ed. Engl.* **1975**, *14*, 745.
(3) Harding, L. B.; Goddard, W. A., III *J. Am. Chem. Soc.* **1978**, *100*, 7180.
(4) Lattimer, R. P.; Kuczkowski, R. L.; Gilles, C. W. *J. Am. Chem. Soc.* **1974**, *96*, 348. Fong, G. D.; Kuczkowski, R. L., *Ibid.*, to be published.
(5) Lovas, F. J.; Suenram, R. D. *Chem. Phys. Lett.* **1977**, *51*, 453. Suenram, R. D.; Lovas, F. J. *J. Am. Chem. Soc.* **1978**, *100*, 5117.
(6) Bailey, P. S.; Thompson, J. A.; Shoulders, B. A. *J. Am. Chem. Soc.* **1966**, *88*, 4098.
(7) Durham, L. J.; Greenwood, F. L. *J. Chem. Soc., Chem. Commun.* **1967**, 843; *J. Org. Chem.* **1968**, *33*, 1629.
(8) Hull, L. A.; Hisatsune, I. C.; Heicklen, J. *J. Am. Chem. Soc.* **1972**, *94*, 4856.
(9) Alcock, W. G., Mile, B. *J. Chem. Soc., Chem. Commun.* **1976**, 5; **1973**, 575.
(10) Nelander, B.; Nord, L. *J. Am. Chem. Soc.* **1979**, *101*, 3769.
(11) Mile, B.; Morris, Gareth W.; Alcock, W. G. *J. Chem. Soc. Perkin Trans. 2* **1979**, 1644.
(12) Nelander, B.; Nord, L. *Tetrahedron Lett.* **1977**, *32*, 2821.
(13) Andrews, L. *J. Chem. Phys.* **1968**, *48*, 972; **1971**, *54*, 4935.

0002-7863/81/1503-2578$01.25/0

Table I. Absorptions (cm^{-1}) Observed in Low-Temperature Reactions of Ethylene and Ozone[a]

neat film[b]	CO_2 matrix[c]	Xe matrix
(410)[d]	406	409
650	648	647
687		686
730	727	727
(850)[d]		846
927	926	927
983	982	983
1214		1214

[a] SOZ absorptions were observed in all of these studies. The 1125 cm^{-1} neat film band attributed to the POZ is in fact due to the SOZ. [b] Reference 8. [c] Reference 12. [d] Estimated from reported spectrum.

Beckman IR-12 spectrophotometer over the range 200–4000 cm^{-1}. Regions of interest were examined by using expanded wavenumber scales; reported band measurements are accurate to ±1 cm^{-1}. The temperature of the CsI cold window was measured by using a Chromel/Au (0.07% Fe) thermocouple attached to the OFHC copper window mount and a potentiometer (Leeds and Northrup Co., Philadelphia). Calibration of this room-temperature reference thermocouple was achieved with the use of the H_2 vapor pressure gauge attached to the block and liquid N_2. Selected samples were photolyzed by using a BH-6 high-pressure mercury-arc lamp (1000 W, General Electric Co. and Illumination Industries, Inc.) for 1-h periods with a 10 cm water filter (to avoid heating the matrix during photolysis), which provided a 220–1000-nm output. A quartz window, sealed with halocarbon wax, allowed access to the matrix.

Chemicals. Ozone was generated by a static electric discharge (Tesla coil) of oxygen in a Pyrex tube and collected by using liquid N_2.[14] The normal isotopic O_2 was obtained from Burdett, U.S.P. grade. Two ^{18}O-enriched samples, obtained from Yeda R&D Co., Ltd. (Israel), were reported as ^{18}O, 50.35% and ^{18}O, 95.57%. Residual O_2 was removed from the O_3 samples by pumping with an oil diffusion pump. The ethylene was obtained from Matheson (C.P. grade). Isotopic ethylene samples obtained from Merck Sharp and Dohme (Montreal) included C_2D_4 (99% D), CH_2CD_2 (98% D_2), and $^{13}C_2H_4$ (90% ^{13}C). All ethylene samples were condensed at 77 K and pumped with an oil diffusion pump to remove any air impurities. Xenon (Airco, purified, 99.9%) was used as received.

Procedure. Ozone and ethylene samples were diluted with matrix gas and codeposited through separate spray-on lines. Several matrix materials (Ar, Kr, Xe, CO_2) and various M/R ratios (50/1, 100/1, 200/1) were tried, but Xe, at 50/1, yielded the best results. Twenty-two xenon experiments were performed to optimize condensation rates and temperature and warming technique to maximize the product absorption yield. The reagents diluted in xenon were codeposited on a CsI window held at 45–50 K; colder deposition temperatures resulted in a more crystalline matrix which cracked and peeled. The temperature was maintained by controlling the voltage through three heater buttons (Minco Products, Inc., Minneapolis) on the window mount while operating the refrigeration system. About 10 mmol of each reagent mixture was deposited at about 2 mmol/h. The warming cycles were performed by shutting off the heaters and the refrigeration system; best results were obtained by allowing the window to warm to about 80 K and recool to 45–50 K over a 25-min period. The warming–cooling cycles greatly decreased the transmission of the matrix, especially above 2000 cm^{-1}.

Results

The infrared spectra of ozonides produced by diffusion and reaction of ethylene and ozone in solid xenon are illustrated in Figure 1. The top trace, Figure 1a , shows the spectrum of Xe/C_2H_4 = 100/1 and Xe/O_3 = 100/1 samples codeposited at 50 K for 5 h; the ethylene and ozone absorptions are labeled E and O_3, respectively. Upon cycling this sample to 80 K over a 10-min period, these absorptions were replaced by new product absorptions, shown in Figure 1b, which are listed in Table I (POZ) and Table II (SOZ). In a more concentrated experiment, 50/1 samples were deposited for 10 h, and weak SOZ, POZ, and formaldehyde product bands were observed after deposition of the two mixtures; after cycling the sample to 50 K over a 12-min period, the spectrum in Figure 1c was recorded. The product bands, labeled S for SOZ and P for POZ, were substantially more intense in the more concentrated experiment, which did not consume all of the reagent molecules. New absorptions were observed for formaldehyde at 1724 cm^{-1} and ethylene oxide, labeled EO, at 865 cm^{-1}. Further sample warming to 100 K increased the SOZ, POZ, and formaldehyde band absorbances with approximately the same relative yields.

The SOZ spectrum in solid argon is contrasted in Figure 1d with the composite SOZ and POZ spectra in xenon matrices to aid identification of the POZ. Ethylene and ozone were condensed with CF_3Cl (Freon 13) in a stainless steel U-tube at −196 °C and allowed to react at −130 °C; the mixture was evacuated at −98 °C to remove solvent and reagents; the residual SOZ was evaporated at −78 °C and condensed with excess argon at 15 K for 2 h.[15] The SOZ absorptions in solid argon, which agree with those reported by Kuhne and Gunthard,[16] are contrasted in Table II with the present xenon matrix SOZ observations.

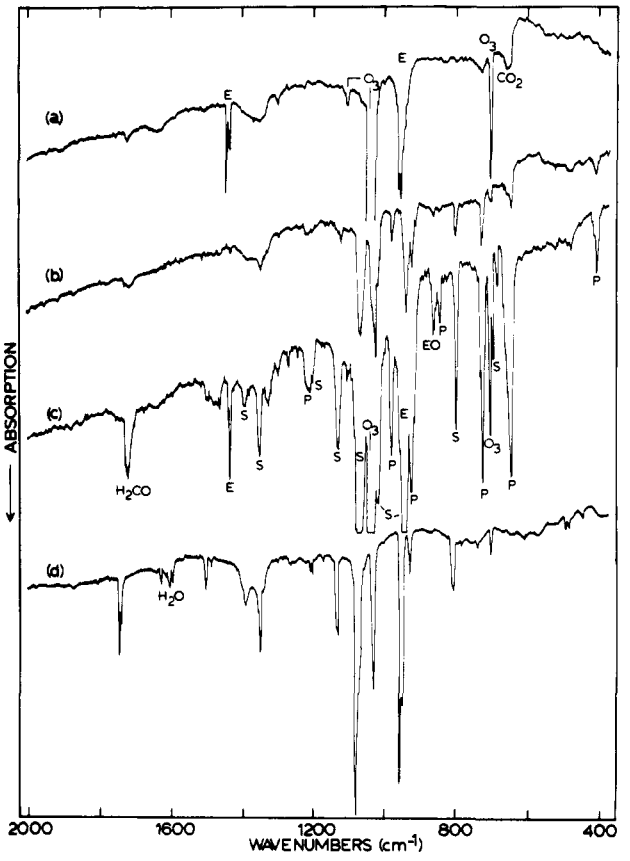

Figure 1. (a) Infrared spectrum of Xe/O_3 = 100/1 and Xe/C_2H_4 = 100/1 samples codeposited at 50 K. (b) Same as (a) after warming to 85 K and cooling to 50 K. (c) Same as (b) but using more concentrated C_2H_4 and O_3 (50/1) and longer sample deposition times. (d) Infrared spectra of the liquid phase ozonolysis products of ethylene in an argon matrix. P = primary ozonide, E = ethylene, EO = ethylene oxide, S = secondary ozonide, and O_3 = ozone.

Table II. Major Absorptions (cm^{-1}) Observed for the Secondary Ozonide of Ethylene (SOZ) Prepared in Freon 13 and Condensed in Argon and Formed by Reaction of Ozone and Ethylene in Solid Xenon

$C_2H_4 + {}^{16}O_3$		$C_2H_4 + {}^{18}O_3$		$^{13}C_2H_4 + {}^{16}O_3$	
Ar	Xe	Ar	Xe	Ar	Xe
806	802	764	760	805	800
952	945	938	930	934	926
1030	1021	1014	1006	1009	999
1079	1072	1053	1047	1059	1052
1130	1130	1125	1127	1119	1122

(14) Andrews, L.; Spiker, R. C. *J. Phys. Chem.* **1972**, *76*, 3208.

(15) Kohlmiller, C. K.; Andrews, L., to be published.

(16) Kuhne, H.; Gunthard, Hs. H. *J. Phys. Chem.* **1976**, *80*, 1238.

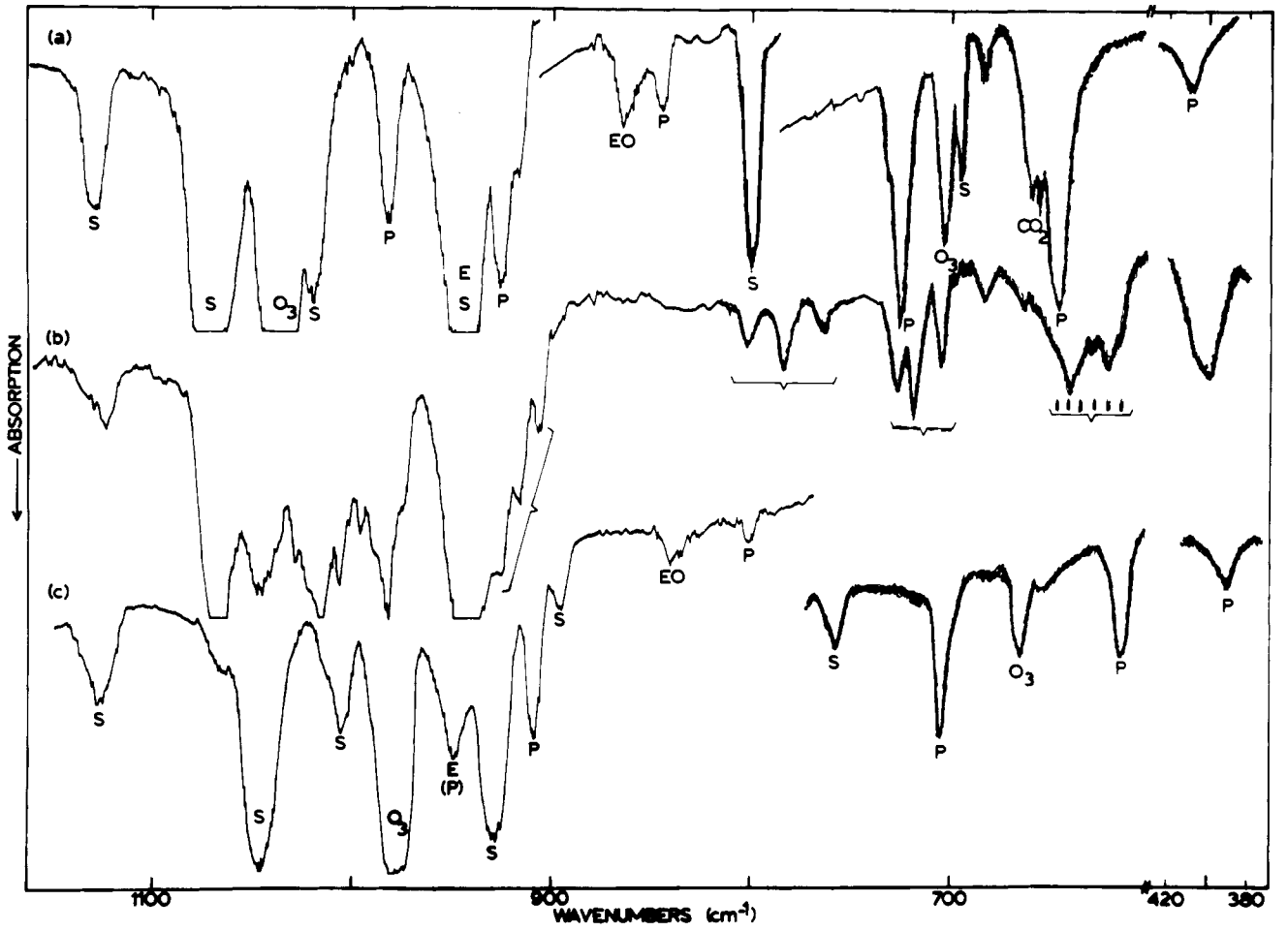

Figure 2. (a) Infrared spectrum of ethylene–ozone reaction products formed during warming codeposited Xe/O_3 = 50/1 and Xe/C_2H_4 = 50/1 samples to 85 K in 20 min. (b) Same as (a) but using $^{16,18}O_3$ (50% oxygen-18) and warming to 85 K then to 95 K. (c) Same as (a) but using $^{18}O_3$ (95% oxygen-18), $Xe/^{18}O_3$ = 100/1, and Xe/C_2H_4 = 100/1 and warming to 80 K for 30 min.

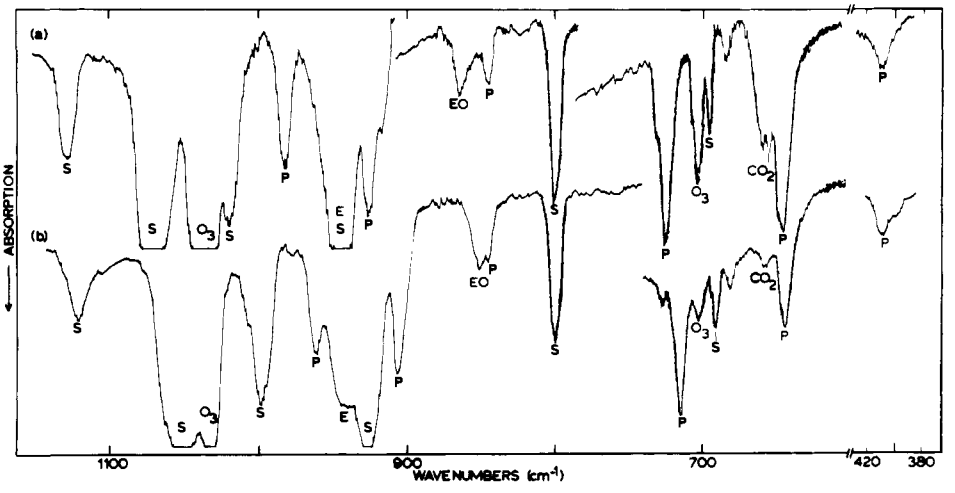

Figure 3. (a) Infrared spectrum of ethylene–ozone reaction products formed during warming codeposited Xe/O_3 = 50/1 and Xe/C_2H_4 = 50/1 samples to 85 K in 20 min. (b) Same as (a) but using $^{13}C_2H_4$ (90% carbon-13) and warming to 85 K and then to 100 K.

Several xenon samples were photolyzed with the high-pressure mercury arc. Photolysis of the sample whose spectrum is shown in Figure 1c with full arc (220–1000 nm) radiation decreased SOZ bands 50–60%, decreased POZ bands 75–85%, doubled the ethylene oxide band at 865 cm^{-1}, and increased broad CH_2O absorptions at 1724, 1501, 1300, and 1175 cm^{-1} and CO_2 at 663 cm^{-1} by an order of magnitude; the 686-cm^{-1} band was unchanged. In another experiment Pyrex-filtered (290–1000 nm) radiation decreased the SOZ bands about 10% and decreased the POZ bands 30–40% without much change in the CH_2O and CO_2 absorptions; again the 686-cm^{-1} band was unchanged.

After establishing the best reaction conditions for maximum product yield with natural isotopic reagents, enriched reagents were employed. At least two and as many as seven experiments were performed with each isotopic sample. The POZ product band positions are listed in Table III for the six isotopic combinations.

Oxygen isotopic spectra are contrasted in Figure 2. Comparison of the $^{16}O_3$ and $^{18}O_3$ spectra in Figures 2a and 2c reveals obvious $^{18}O_3$ counterparts at 390, 615, 705, 802, and 908 cm^{-1} for the $^{16}O_3$ product bands at 409, 647, 727, 846, and 927 cm^{-1}, respectively. The $^{18}O_3$ counterpart of the 983-cm^{-1} band is probably obscured by the 955-cm^{-1} E band. The scrambled ozone

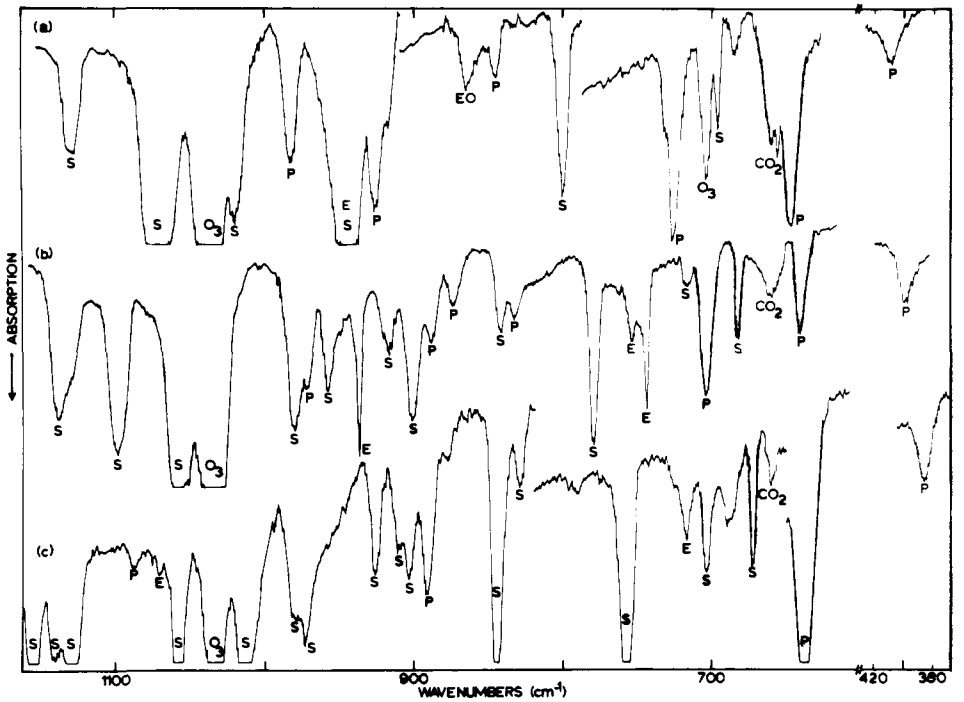

Figure 4. (a) Infrared spectrum of ethylene–ozone reaction products formed during warming codeposited Xe/O_3 = 50/1 and Xe/C_2H_4 = 50/1 samples to 85 K in 20 min. (b) Same as (a) but using CH_2CD_2. (c) Same as (a) but using C_2D_4 and warming to 110 K in 24 min.

Table III. Isotopic Absorptions (cm^{-1}) for Primary Ozonides of Ethylene and Ozone (POZ) in Solid Xenon at 50 K

$C_2H_4 + {}^{16}O_3$	$C_2H_4 + {}^{16,18}O_3$	$C_2H_4 + {}^{18}O_3$	$CH_2CD_2 + {}^{16}O_3$	$C_2D_4 + {}^{16}O_3$	${}^{13}C_2H_4 + {}^{16}O_3$
409	400 (br)	390	398	387	408
647	647, 641, 636, 630, 623, 616	615	641	636	644
727	727, 719, 705	705	(704)		716
846		802			846
927	927, 917, 909	909	a	892	906
983		(955)	a		961
1214	1210 (br)	1208	1210	1089	1210

[a] Absorptions were observed at 974, 889, 874, and 833 cm^{-1} believed to be due to the POZ-d_2; however, due to the lowered symmetry and interaction between H–C–H bending and C–O stretching modes, no assignment can be made.

experiments were complicated by isotopic dilution over six precursor and six of each product isotopic molecule, which prevented definitive measurements in the upper 900-cm^{-1} region. However, a triplet was partially resolved at 927, 917, and 908 cm^{-1} on the side of a strong S band, and a sharp triplet was resolved at 727, 719, and 705 cm^{-1} in Figure 2b. A partially resolved sextet was observed at 647, 641, 636, 630, 623, and 616 cm^{-1} and a broad band was found centered at 400 cm^{-1}. These observations were reproduced in two other 50% oxygen-18 enriched ozone experiments.

The infrared spectrum for the ${}^{13}C_2H_4$ reaction with ozone is compared with the ${}^{12}C_2H_4$ spectrum in Figure 3. This sample was first cycled to 85 K and then to 100 K; the latter cycle, illustrated in Figure 3b, increased the product bands by 20%. A straightforward mapping with the ${}^{12}C_2H_4$ reaction products gives the POZ absorptions listed in Table III. The SOZ was prepared with ${}^{13}C_2H_4$ in Freon to further confirm the identity of SOZ bands, which are compared in Table II. The POZ band at 961 cm^{-1} was observed on the side of the strong ${}^{13}E$ band at 946 cm^{-1}, and the POZ band at 846 cm^{-1} was observed as a shoulder on the ${}^{13}EO$ band displaced to 852 cm^{-1}. The strong 716 cm^{-1} product band (A = 0.58) exhibited a 727-cm^{-1} satellite band (A = 0.06) at the same frequency observed in the ${}^{12}C_2H_4$ studies.

Infrared spectra for reactions between O_3 and C_2H_4, CH_2CD_2, and C_2D_4 are compared in Figure 4. Again the SOZ bands were identified from samples reacted in CF_3Cl solution.[15] Only two absorptions in the C_2H_4 experiments can be clearly tracked through the deuteration sequence in Figure 4a–c; the strong 647-cm^{-1} absorption exhibits counterparts at 641 and 636 cm^{-1} and the 409-cm^{-1} band has d_2 and d_4 counterparts at 398 and 387 cm^{-1}, respectively. The strong 704-cm^{-1} band in the d_2 experiment, Figure 4b, coincides with O_3, but since the 704-cm^{-1} band broadened while the sharp 704-cm^{-1} O_3 absorption decreased, some POZ absorption may be concealed. Finally, no d_4 or h_4 SOZ species were observed in the CH_2CD_2 experiments as shown by the absence of the strong 802 cm^{-1} h_4 band and the strong 1156 cm^{-1} d_4 band. The C_2D_4 sample was cycled to 110 K which produced a very large product yield. The strong SOZ band at 846 cm^{-1} may also obscure a weaker POZ absorption. In addition to the two d_4 counterpart bands mentioned above, the only other POZ-d_4 band was observed at 892 cm^{-1}. Photolysis of this sample again virtually destroyed the POZ bands and substantially decreased the SOZ absorptions.

One experiment was performed with Kr/O_3 = 100/1 and Kr/C_2H_4 = 100/1 samples codeposited at about 35 K. No reaction of ethylene and ozone was observed during condensation nor upon temperature cycling to 50 and 59 K. However, a temperature cycle to 67 K produced a weak new 1073-cm^{-1} band, which corresponds to the strongest SOZ absorption observed at 1078 cm^{-1} in solid argon and 1072 cm^{-1} in solid xenon. Further warming of the krypton sample removed reagent absorption without increasing the reaction product, presumably owing to sample evaporation.

Several Ar/O_3 = Ar/C_2H_4 = 200/1 experiments were done codepositing samples at 15 K. Again, no reaction was observed during condensation. Since the above experiments demonstrated that temperatures in excess of 70 K are required for appreciable reaction of ethylene and ozone, no warming cycles were performed as the argon matrix will rapidly evaporate above 50 K. The argon samples were photolyzed with the full mercury arc; the major product was the ethylene oxide 878-cm^{-1} absorption.

Two carbon dioxide matrix experiments were performed, as first reported by Nelander and Nord.[12] The best one of these was comparable to the product yield in Figure 1b, except that the 600-cm^{-1} region was obscured by the matrix absorption. Since xenon proved to be the superior matrix for product yield, as shown by comparison with Figure 1c, and the goal of these studies was oxygen isotopic substitution, which could be complicated by ex-

Table IV. Observed and Calculated Carbon-13 and Oxygen-18 Isotopic Shifts and Vibrational Assignments for Major Primary Ozonide Absorptions Based upon Diatomic C–O and O–O Approximations

12-16 obsd	13-16 calcd	13-16 obsd	18-18 calcd	12-18 calcd	12-18 obsd	assignment
409	400	408	386	399	390	O–O–O bend
647	633	644	610	631	615	antisym O–O–O str
727	711	716	685	709	705	C–O–O bend, C–O str
846	827	846	798	826	802	sym O–O–O str
927	906	906	874	905	909	C–O str
983	961	961	927	959	(955)	C–O str, H–C–H bend
1214	1187	1210	1145	1185	1208	H–C–H bend

change with a CO_2 matrix, no further work was attempted with carbon dioxide.

Discussion

Absorptions which can be assigned to the primary ozonide of ethylene will be identified, their vibrational assignments will be made based upon isotopic data, and bonding in the molecule will be considered in light of the infrared spectrum.

Identification. The new absorptions listed in Table I were produced by the reaction of ozone and ethylene in solid xenon, solid carbon dioxide, and neat solid films; the absorption positions agree within small variations for the different environments. Seven of the bands exhibited constant relative intensities during growth upon sample warming and decrease upon photolysis, which is a necessary condition for their assignment to the same molecule. On the other hand, the 686-cm^{-1} band remained on photolysis and did not track with the POZ band growth on warming to 100 K; the weak 686-cm^{-1} band is due to a different, less-reactive species.

The seven product bands were produced in lower yield than SOZ bands in the xenon experiments, and the former bands were more photosensitive than the SOZ bands. Finally, the Freon solution reaction product was exclusively SOZ which identifies SOZ absorptions in the xenon experiments and demonstrates that the seven bands in Table I are due to a different reaction product. All of this evidence is consistent with the primary ozonide **1** as the species responsible for the absorptions in Table I, as proposed by two earlier groups.[8,12]

The strong POZ absorption at 647 cm^{-1} reveals the stoichiometric composition of the POZ species from isotopic data obtained in the present experiments. The minor involvement of carbon in this mode is demonstrated by the 3-cm^{-1} carbon-13 shift, and minimal interaction with CH_2 groups is shown by the 647, 641, and 636 cm^{-1} pattern in the C_2H_4, CH_2CD_2, and C_2D_4 reactions. Of most importance, the 647-cm^{-1} band splits into a partially resolved, evenly spaced sextet in the 50% oxygen-18 enriched ozone experiment, illustrated in Figure 2. Even though this sextet is not as well resolved as those reported for alkali metal ozonides,[17] the 1/2/1/1/2/1 relative intensity band profile of evenly spaced components is clearly apparent. The major features at 641 and 623 cm^{-1}, due to the 16–16–18 and 16–18–18 isotopic species, are displaced from the pure isotopic components at 647 and 615 cm^{-1}. The large oxygen-18, small carbon-13, and small CD_2 isotopic shifts observed for the 647-cm^{-1} band characterize an essentially pure O–O stretching mode, as will be discussed below. The sextet absorption for the O–O stretching mode, therefore, verifies the two-equivalent plus one-inequivalent adjacent oxygen atom or ozonide structure **1** for the POZ. Although the strong 1079-cm^{-1} SOZ band also exhibits a mixed oxygen isotopic sextet, this band is a "doublet of triplets" showing a major dependence on one oxygen and a minor dependence on two equivalent oxygen atoms;[15] the intermediate oxygen-18 and carbon-13 isotopic shifts for the 1079-cm^{-1} band characterize a C–O stretching mode, and the SOZ structure **3** is compatible with the isotopic observations. The participation of separated single and paired oxygen atoms in a vibrational mode clearly requires the involvement of carbon in the SOZ arrangement; however, the lack of major involvement of carbon in the 647-cm^{-1} absorption, which splits into an oxygen isotopic sextet, requires the three adjacent oxygen POZ arrangement. These isotopic observations, accordingly, confirm the POZ identification in the xenon matrix experiments.

Table V. Fundamental Vibrations (cm^{-1}) for Ozone, Ozonides, and Trioxides

molecule	O–O–O bend	antisym O–O–O str	sym O–O–O str
O_3[a]	704	1040	1104
O_3^- [b]	600	804	1016
$(CF_3)_2O_3$[c]	288	773	875
POZ[d]	409	647	846

[a] Reference 14. [b] Reference 17. [c] Reference 18. [d] This work.

Vibrational Assignments. A qualitatively accurate characterization of the POZ normal modes can be obtained from the isotopic shifts, particularly the oxygen-18 and carbon-13 displacements. A simple comparison between the calculated and observed isotopic shifts assuming a diatomic C–O or O–O vibration provides substantial information about the normal modes, as can be seen from Table IV.

First, the 409-, 647-, 846-cm^{-1} bands exhibit large oxygen-18, small carbon-13, and small CD_2 shifts. These are predominantly oxygen vibrations, although in the POZ molecule, the O–O vibrations must exhibit a slightly smaller oxygen-18 shift than calculated, that is a smaller 16/18 ratio than ozone itself, owing to minor participation of the adjacent CH_2 groups. The isotopic ratio for ozone, 1040.0/982.8 = 1.0582, and the analogous POZ ratio, 647/615 = 1.052, attest this point.

The relative intensities and positions among the three fundamentals[14,17] for O_3 and O_3^-, compared in Table V, show that the weak 846-cm^{-1} band is due to the symmetric O–O–O stretching mode, the strong 647-cm^{-1} absorption arises from the antisymmetric O–O–O stretching mode, and the lower frequency, medium intensity band at 409 cm^{-1} is due to the O–O–O valence angle bending mode. A similar comparison can be made with the spectrum of CF_3–O–O–O–CF_3.[18]

The 927-cm^{-1} absorption exhibits the expected ^{18}O and ^{13}C shifts for a C–O stretching mode; even the displacement with C_2D_4 is comparatively small showing little H(D) involvement in this mode. The 927-cm^{-1} band splits into three components in the mixed oxygen isotopic compound indicating that this vibration involves the two equivalent C–O groups in the POZ molecule.

The 727-cm^{-1} band also exhibits a triplet splitting in the $^{16,18}O_3$ experiments; however, the ^{13}C shift of 11 cm^{-1} falls short of the 17 cm^{-1} calculated whereas the observed ^{18}O shift of 22 cm^{-1} exceeds the 18 cm^{-1} prediction for a C–O vibration. Furthermore, the observation of the 716-cm^{-1} 716-cm^{-1} carbon-13 and 727-cm^{-1} carbon-12 counterparts with 9/1 relative intensity using a 90% carbon-13 enriched sample shows that one carbon is involved in this mode. The 727-cm^{-1} band is best characterized as the C–O–O bending mode with some C–O stretching character involving a common carbon; inequivalence between the two oxygen atoms was not resolved in the spectrum.

The 983-cm^{-1} band exhibits the proper carbon-13 shift for a C-O stretching mode, and although the oxygen-18 counterpart was not found, it was probably obscured by ethylene. The fact that d_2 and d_4 counterparts could not be found for the 983-cm^{-1} band also infers some H–C–H bending character for this mode. The 1214-cm^{-1} POZ absorption shows small oxygen-18 and carbon-13 displacements that are indicative of an H–C–H bending mode; a possible D–C–D counterpart was observed at 1089 cm^{-1}. The xenon matrices were nearly opaque in the C–H stretching region and no absorptions could be observed under these conditions.

(17) Spiker, R. C.; Andrews, L. *J. Chem. Phys.* **1973**, *59*, 1851, 1863.

(18) Witt, J. D.; Durig, J. R.; Des Marteau, D.; Hammaker, R. M. *Inorg. Chem.* **1973**, *12*, 807.

The vibrational assignments based upon carbon-13, oxygen-18, and deuterium isotopic shifts are in general agreement with those of Alcock and Mile[9] that C-O stretches for the POZ fall in the 900–1000-cm^{-1} range and that the strong O–O–O stretching mode is substantially lower (697 cm^{-1} in the case of diisopropylethylene ozonide) based on comparisons with cyclic ethers and peroxides[9] and on very recent unpublished oxygen-18 substitution results.[11] These assignments are in disagreement with the tentative ones of Hull et al.[8] based on a simple comparison with ozone. Clearly, carbon-13 and oxygen-18 isotopic data are needed to make correct vibrational assignments.

Bonding in the Primary Ozonide. The most interesting part of the POZ molecule is the -O-O-O- group, and information on the binding in this group can be obtained through comparison to similar molecules containing the trioxygen linkage. Table V shows that the O–O stretching modes for the POZ are substantially lower than ozone, inorganic ozonide, and bis(trifluoromethyl)trioxide values. This comparison shows that the O–O–O bonds in the POZ are comparatively weak σ bonds, particularly relative to the "standard" O–O single bond fundamental at 880 cm^{-1} in hydrogen peroxide.[19] The instability of the POZ to decomposition by rupture of an O-O bond is also indicative of weak O-O bonds.

On the other hand, the C-O stretching modes of the POZ, 983 and 927 cm^{-1}, are just below the strong C-O stretching modes of the SOZ at 1079 and 952 cm^{-1} and the C-O stretching mode of CH_3OH at 1034 cm^{-1},[20] which shows that the C-O bonds in the POZ are only slightly weaker than normal single bonds.

Reactions Occurring in Solid Xenon. Finally, the reaction of ethylene and ozone proceeds at a finite rate in solid xenon at 80 K. Nelander and Nord have shown that the rate of formation of POZ in solid CO_2 is consistent with a 4 ± 1 kcal/mol activation energy, in agreement with the gas-phase value.[12] The POZ is believed to be formed by a concerted reaction; indirect support for the concerted mechanism may be derived from the failure to observe any additional absorptions in the xenon experiments that might be due to a $\cdot CH_2CH_2OOO\cdot$ intermediate. Rearrangement of POZ to SOZ occurs within the matrix cage as is shown by the lack of h_4 and d_4 SOZ species in the CH_2CD_2 experiments. Although formaldehyde was a major reaction product, no evidence was found for additional transient species such as dioxirane or methylene peroxide.

The relative yields of the several reaction products were not changed with reaction temperature in different experiments. Based on the SOZ and POZ band absorbances at 802 and 727 cm^{-1}, respectively, a comparable yield of each species was produced, and there was no measurable difference in the relative SOZ and POZ yields for reaction in the 80–100 K range. Since the warming-cooling cycles decreased sample transmission and photometric accuracy, a very small change (<10%) in the relative SOZ and POZ yields over this limited temperature range cannot be determined.

Conclusions

Ozone and ethylene react upon diffusion at approximately 80 K in solid xenon to form the POZ and SOZ products. The latter absorptions were identified by preparing the SOZ species in Freon solution for matrix spectroscopic study; the remaining POZ absorptions were more photosensitive than the SOZ bands. Isotopic substitution ($^{16,18}O_3$, $^{18}O_3$, CH_2CD_2, C_2D_4, and $^{13}C_2H_4$) provides a sound basis for characterizing the POZ vibrational modes. The C-O stretching vibrations at 983 and 927 cm^{-1} are reasonable values for single bonds; however, the symmetric and antisymmetric O-O-O stretching modes at 846 and 647 cm^{-1}, respectively, are unusually low values for single bonds, consistent with the instability of the POZ species to O–O bond rupture. A 1/2/1/1/2/1 relative intensity sextet for the strong 647-cm^{-1} band in the 50% oxygen-18 enriched experiment confirms the POZ structural arrangement.

Acknowledgement is made to the donors of the Petroleum Research Fund, administered by the American Chemical Society, for support of this research.

(19) Redington, R. L.; Olson, W. B.; Cross, P. C. *J. Chem. Phys.* **1962**, *36*, 1311.
(20) Herzberg, G. "Infrared and Raman Spectra"; D. Van Nostrand: New York, 1945; p 335.

Secondary Ion Mass Spectra of Coordination Compounds and Organometallics

Janelle Pierce, Kenneth L. Busch, R. A. Walton,* and R. G. Cooks*

Contribution from the Department of Chemistry, Purdue University, West Lafayette, Indiana 47907. *Received October 20, 1980*

Abstract: The extension of secondary ion mass spectrometry (SIMS) to the direct analysis from surfaces of preformed, well-defined, coordination compounds and organometallics is presented. In both instances, the SIMS spectra contain ions characteristic of molecular weight and structurally diagnostic fragment ions. Secondary ions are produced by several mechanisms, including cationization, electron transfer, and direct sputtering of precharged species. Ammonium chloride and sodium chloride were investigated as room-temperature matrices to decrease the abundances of ions resulting from intermolecular processes and increase the S/N ratio for peaks corresponding to structurally informative ions. Empirical structure–spectral correlations developed in this study aid in the definition of surface structure on a scale particularly appropriate to catalysis research.

The unique catalytic properties of many transition-metal complexes have provided some of the impetus for the synthesis of increasingly complex molecules. Mass spectrometry has been used extensively in the characterization of such compounds[1] and continued expansions and refinements of the technique have been chronicled in regular reviews.[2,3] Since many coordination complexes and organometallic compounds are prone to thermal decomposition, methods which avoid macroscopic vaporization of the sample, such as field desorption and plasma desorption mass spectrometry, have seen some application in this area. Use of a surface analysis technique such as secondary ion mass spectrometry (SIMS) can also obviate such a requirement. Recent applications of SIMS to the analysis of organic compounds[4] have revealed that stable gas-phase complexes, such as those between transition metals

(1) Litzow, M. R.; Spalding, T. R. "Mass Spectrometry of Inorganic and Organometallic Compounds"; Elsevier: New York, 1973.
(2) Spalding, T. R. In "Mass Spectrometry"; Johnstone, R. A. W., Ed.; The Chemical Society: London, 1979; Vol. 5.
(3) Burlingame, A. L.; Baillie, T. A.; Derrick, P. J.; Chizhov, O. S. *Anal. Chem.* **1980**, *52*, 214R.

0002-7863/81/1503-2583$01.25/0